Food Chemistry: X 14 (2022) 100286

Contents lists available at ScienceDirect

Food Chemistry: X

journal homepage: www.sciencedirect.com/journal/food-chemistry-x

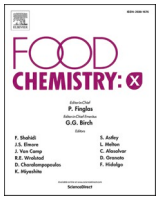

Four cucurbitane glycosides taimordisins A–D with novel furopyranone skeletons isolated from the fruits of *Momordica charantia*

Chia-Ching Liaw [a,b], I-Wen Lo [c], Yu-Chi Lin [a], Hung-Tse Huang [a], Li-Jie Zhang [a], Pin-Chun Hsiao [a], Tsung-Lin Li [c,*], Yao-Haur Kuo [a,d,e,*]

[a] *Division of Chinese Material Medica Development, National Research Institute of Chinese Medicine, Taipei 112026, Taiwan*
[b] *Department of Biochemical Science and Technology, National Chiayi University, Chiayi 600355, Taiwan*
[c] *Genomics Research Center, Academia Sinica, Taipei 115201, Taiwan*
[d] *Graduate Institute of Integrated Medicine, College of Chinese Medicine, China Medical University, Taichung 404333, Taiwan*
[e] *Taoyuan 327008, Taiwan*

ARTICLE INFO

Keywords:
Momordica charantia
Cucurbitane
Taimordisins
Anti-inflammatory
NO production

ABSTRACT

Four novel triterpene glycosides, taimordisins A–D (**1**–**4**), were discovered from fresh fruits of Taiwanese *Momordica charantia*. The chemical framework and relative stereochemistry of these four natural products were isolated, purified, and determined by using various separation and spectroscopy techniques. Each of them features a unique bicyclic-fused or trifuso-centro-fused ring system. Notably, **1** and **2** are cucurbitane-based compounds possessing a new C-24 and C-2″ carbon–carbon linkage with 5-hydroxy-2-(hydroxymethyl)tetrahydro-4*H*-pyran-4-one and 6-(hydroxymethyl)tetrahydro-4*H*-pyran-3,4,4-triol units, respectively, and represented an unprecedented molecular skeleton. In terms of biosynthesis, they all originate from a common precursor 3-hydroxycucurbita-5,24-dien-19-al-7,23-di-*O*-*β*-glucopyranoside. Of two sugar moieties, the one at 23-*O*-*β*-glucopyranoside grants each individual congener uniqueness likely through microbial symbiont-mediated intramolecular transformation into two major types of furo[2,3-*b*]pyranone and furo[3,2-*c*]pyranone derivatives. These new products possess desirable anti-inflammatory biological activities in addition to being generally regarded as safe.

Introduction

Cucurbitacins are characteristic components existing in cucurbitaceous plants and some other related plant families. They are composed of a highly oxygenated tetracyclic triterpenoid-derived cucurbitane core decorated with multi-heterocyclically rearranged pyranoses (Chen et al., 2005). Fruits of *Momordica charantia* (MC), known as bitter gourds, are vegetables used in many popular dishes or health-promoting tea preparations worldwide. Beyond that, the MC extracts have also been utilized as a folk medicine for thousands of years in many places of the world, especially as a Traditional Chinese Medicine (TCM) for diabetes treatment in China (Chen et al., 2015; Wang et al., 2017). Cucurbitane triterpenoids from MC, often present in glycosides, are known the major bitter substances in different parts of MC (such as vines, leaves, and seeds), and they are prominent for a broad range of pharmacological potentials, especially anti-diabetic (Wang et al., 2014), anti-inflammation (Abdelwahab et al., 2011), anti-cancer (Akihisa et al., 2007; Li et al., 2017), and anti-multidrug resistance against various types of tumor cells (Ramalhete et al., 2016).

As a functional food, MC drew considerable attention in recent years because it is beneficial to several metabolic syndromes, including hyperglycemia, obesity, hypertension, and dyslipidemia (Sung et al., 2018). Of these biological functionalities (Jia et al., 2017), anti-inflammation is relatively less examined, while it deserves one's special attention. Obesity is closely related to type 2 diabetes, in which the obesity-induced chronic adipose tissue inflammation is a critical factor. It has been reported that oral administration of 2% or 5% MC (dry powder) significantly decreased macrophage infiltration in epididymal adipose tissues (EAT) and brown adipose tissues of high-fat dieted rats, downregulated expressions of pro-inflammatory cytokines, MCP-1/CCL2, TNF-α, and IL-6 in EAT (Bao et al., 2013). MC extracts were also reported in a position to reduce secretions of pro-inflammatory

* Corresponding authors at: Genomics Research Center, Academia Sinica, Taipei 115201, Taiwan (T.L. Li). Division of Chinese Materia Medica Development, National Research Institute of Chinese Medicine, Taipei 112026, Taiwan (Y.H. Kuo).
E-mail addresses: tlli@gate.sinica.edu.tw (T.-L. Li), kuoyh@nricm.edu.tw (Y.-H. Kuo).

https://doi.org/10.1016/j.fochx.2022.100286
Received 22 December 2021; Received in revised form 14 March 2022; Accepted 14 March 2022
Available online 16 March 2022

cytokines but instead promote secretions of anti-inflammatory cytokines TGF-β and IL-10, leading to attenuation of inflammatory stress and decrease of lymphocytes by suppressing activation of NF-KB signaling pathway in mouse models of leukemia and sepsis (Manabe et al., 2003; Chao et al., 2014).

In our recent research, fourteen new cucurbitane-type triterpenoids derivatives, kuguaovins A-M, were identified from the vines of MC (Huang et al., 2020; Liaw et al., 2022) with their anti-inflammatory, cytotoxic, and anti-diabetic activity. We are continuing our endeavor in discovering small molecules via a medicinal chemistry approach. In this report, we discovered four novel momordicine glycosides, taimordisins A–D (**1**–**4**) (Fig. 1), that were isolated and purified to homogeneity from fresh MC fruits. Since the biogenesis of the momordicine aglycone that is derived from cucurbitadienol is well documented particularly for the cyclization of 2,3-oxidosqualene by a cucurbitadienol synthase (one of oxidosqualene cyclases, OSCs) (Shibuya et al., 2004) and its subsequent modifications, we put forward plausible biosynthetic routes for these four cucurbitacins. Moreover, we reason that each given bicyclic or tricyclic unit in each individual taimordisins A–D (**1**–**4**) is likely originated from *β*-D-glucose and transformed to either furo[2,3-*b*]pyranone or furo[3,2-*c*]pyranone (Thorat & Kontham, 2021). Finally, we report their biological evaluation on anti-inflammation in addition to the determination of chemical structures of these four new MC isolates.

Material and methods

General experimental procedures

Optical rotations and infrared (IR) spectra were measured by a JASCO P-2000 polarimeter and Mattson Genesis II spectrophotometer, respectively. The 1D (^{1}H and ^{13}C) and 2D (^{1}H–^{1}H COSY, HMQC, HMBC, and NOESY) spectra were recorded by Bruker Avance 400 MHz and Varian VMNRS-600 using CD_3OD (methanol-d_4, Merck) or C_5D_5N (pyridine-d_5, Merck). Electrospray ionization mass spectrometry (ESI-MS) data and high resolution electrospray ionization mass spectrometry (HR-ESI-MS) data of samples in methanol were respectively measured on a VG Biotech Quattro 5022 mass spectrometer (VG Biotech, Altrincham, UK) and a Finnigan MAT-95XL mass spectrometer (Thermo). Gas chromatography (GC) data was carried out using a 6890N network GS system (Agilent) using a Chirasil-L-Val column (25 m 0.22 mm) with He as carrier gas. Diaion HP-20 (Mitsubishi Chemical Co.), Sephadex LH-20 (GE), and silica gel 60 (Merck, 70–230 and 230–400 mesh) resins were used for column chromatography, whereas pre-coated silica gel plates (Merck, Kieselgel 60 F_{254}, 1 mm) were used for thin-layer chromatography (TLC). The components were preliminarily distinguished detected on TLC by heating at 100 °C and sprayed with anisaldehyde-sulphuric acid reagent (5% H_2SO_4). HPLC purification was performed on a Shimadzu LC-6AD series apparatus with a SPD-10A UV detector (Shimadzu) and/or ELSD detector (Varian, 380-LC), equipped with a 250 × 20 mm or 250 × 4.6 mm preparative Cosmosil 5C_{18} AR-II column (Nacalai Tesque, Inc.). The absorbance at selected wavelengths was measured by using a spectrophotometric plate reader (DYNEX Technologies, USA).

Plant material

The fresh fruits of Taiwanese *M. charantia* cultivated in Nantou County, Taiwan were provided by Starsci Biotech Co. Ltd. Voucher specimens (NRICM, No. 20090901) have been deposited in the National Research Institute of Chinese Medicine, Taipei, Taiwan.

Extraction, isolation, and purification

The fresh fruits of *M. charantia* (wet, 3.6 kg) were sliced and extracted three times with 70% ethanol (EtOH, 7.0 L) at 50 °C for 24 hr, and then concentrated under reduced pressure. The EtOH extract (75 g) was subjected to an open column chromatography with Diaion HP-20

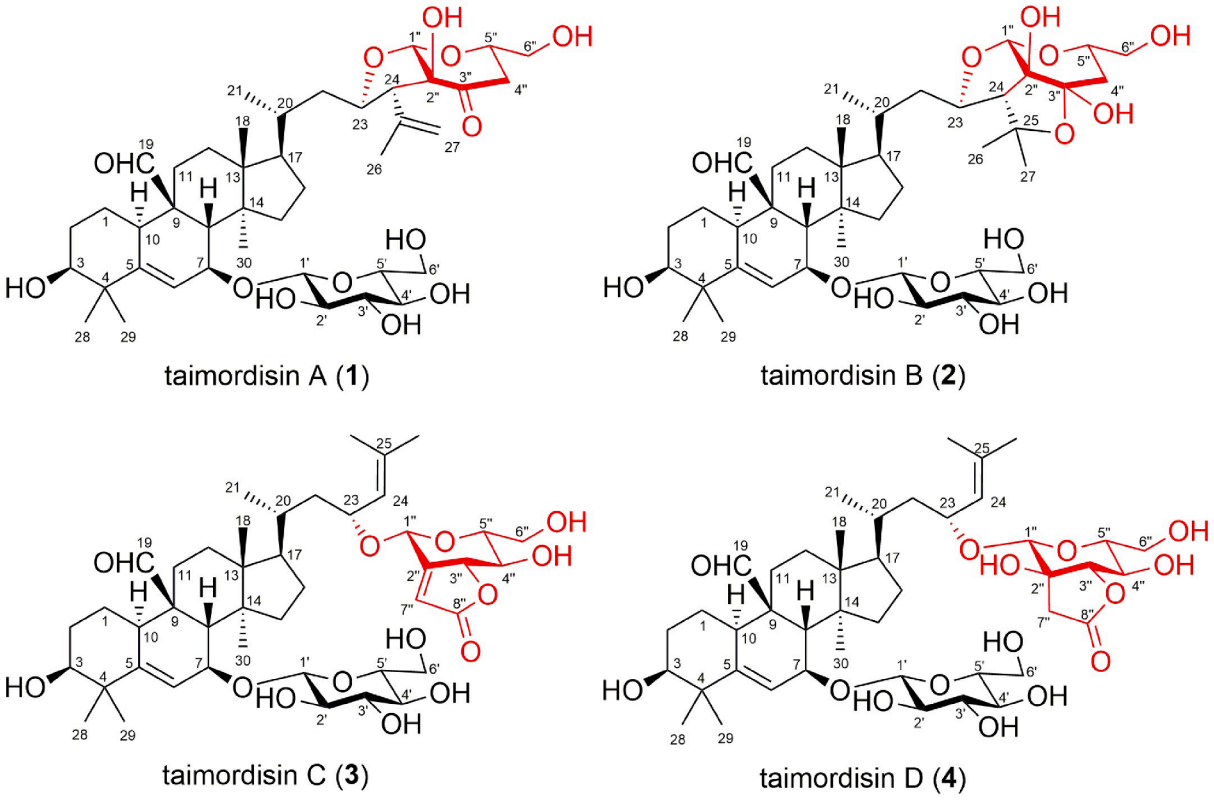

Fig. 1. The chemical structures of compounds **1**–**4** from the fruit of *Momordica charantia*.

Table 1
^{1}H- and ^{13}C NMR data of taimordisins A (**1**) and B (**2**).

No.	**1** (MeOH-d_4)[a]		**1** (Pyridine-d_5)[b]		**2** (Pyridine-d_5)[a]	
	δ_H (*J*, Hz)	δ_C	δ_H (*J*, Hz)	δ_C	δ_H (*J*, Hz)	δ_C
1a	1.48 m	20.2 (CH_2)	1.68 m	22.4 (CH_2)	1.69 m	22.4 (CH_2)
1b	1.59 m		1.93 m		1.93 m	
2a	1.29 m	28.1 (CH_2)	1.93 m	30.3 (CH_2)	1.90 m	30.3 (CH_2)
2b	1.70 m		2.06 m		2.03 m	
3	3.55 br d (4.1)	74.9 (CH)	3.80 br t (2.9)	76.0 (CH)	3.81 br t (4.5)	76.0 (CH)
4		40.3 (C)		42.4 (C)		42.4 (C)
5		145.8 (C)		148.1 (C)		148.2 (C)
6	5.95 br d (4.1)	121.3 (CH)	6.14 br d (3.7)	122.7 (CH)	6.19 br d (3.8)	122.7 (CH)
7	3.27 overlapped	69.5 (CH)	4.61 br d (5.6)	71.7 (CH)	4.64 br d (5.4)	71.8 (CH)
8	2.10 br s	44.7 (CH)	2.53 br s	45.2 (CH)	2.56 br d (4.6)	45.1 (CH)
9		49.2 (C)		50.9 (C)		50.9 (C)
10	2.59 dd (13.8, 4.4)	35.3 (CH)	2.66 overlapped	37.2 (CH)	2.66 overlapped	37.2 (CH)
11a	1.45 m	21.1 (CH_2)	1.57 overlapped	23.1 (CH_2)	1.57 overlapped	23.1 (CH_2)
11b	2.36 m		2.67 overlapped		2.67 overlapped	
12a	1.26 m	27.7 (CH_2)	1.62 m	30.0 (CH_2)	1.63 m	29.9 (CH_2)
12b	2.00 m		1.93 m		1.90 m	
13		44.6 (C)		46.3 (C)		46.3 (C)
14		46.8 (C)		48.8 (C)		48.8 (C)
15a	1.36 m	33.5 (CH_2)	1.47 m	35.3 (CH_2)	1.50 m	35.3 (CH_2)
15b	1.36 m		1.59 m		1.59 m	
16a	1.39 m	26.4 (CH_2)	1.58 m	28.5 (CH_2)	1.41 m	28.5 (CH_2)
16b	1.90 m		2.06 m		1.93 m	
17	1.49 m	50.3 (CH)	1.56 m	51.9 (CH)	1.53 m	51.7 (CH)
18	0.94 s	13.3 (CH_3)	0.92 s	15.5 (CH_3)	0.91 s	15.4 (CH_3)
19	9.85 s	208.1 (CH)	10.50 s	207.8 (CH)	10.51 s	207.7 (CH)
20	1.78 m	31.6 (CH)	2.09 m	33.5 (CH)	1.99 m	34.4 (CH)
21	0.97 d (6.2)	16.7 (CH_3)	1.08 d (6.4)	19.0 (CH_3)	1.04 d (6.3)	19.5 (CH_3)
22a	0.84 m	37.9 (CH_2)	1.16 m	39.7 (CH_2)	1.25 m	44.8 (CH_2)
22b	2.08m		2.52 m		2.08 m	
23	4.65 ddd (11.2, 8.8, 1.6)	78.9 (CH)	4.90 ddd (10.7, 8.4, 1.9)	80.6 (CH)	4.86 ddd (10.6, 5.9, 2.0)	79.9 (CH)
24	3.53 d (8.8)	50.7 (CH)	3.92 d (8.3)	52.8 (CH)	2.64 d (5.9)	66.7 (CH)
25		137.2 (C)		139.7 (C)		81.1 (C)
26	1.74 s	22.7 (CH_3)	1.88 s	25.0 (CH_3)	1.47 s	26.2 (CH_3)
27a	4.91 br s	114.4 (CH_2)	5.11 br s	116.8 (CH_2)	1.77 s	33.4 (CH_3)
27b	5.14 br s		5.63 br s			
28	1.08 s	25.7 (CH_3)	1.14 s	27.8 (CH_3)	1.15 s	27.8 (CH_3)
29	1.25 s	23.9 (CH_3)	1.45 s	26.7 (CH_3)	1.48 s	26.8 (CH_3)
30	0.82 s	16.5 (CH_3)	0.76 s	18.6 (CH_3)	0.78 s	18.6 (CH_3)
1′	4.24 d (7.8)	100.0 (CH)	4.96 d (7.7)	101.8 (CH)	5.01 d (7.7)	101.9 (CH)
2′	3.13 dd (8.7, 7.8)	72.9 (CH)	4.01 overlapped	75.5 (CH)	4.06 dd (8.2, 7.7)	75.5 (CH)
3′	3.33 overlapped	75.9 (CH)	4.32 dd (8.8, 8.7)	79.3 (CH)	4.35 dd (9.1, 8.2)	79.3 (CH)
4′	3.73 overlapped	71.2 (CH)	4.03 dd (8.7, 8.3)	72.4 (CH)	4.30 dd (9.1, 8.8)	72.1 (CH)
5′	3.23 overlapped	76.0 (CH)	4.28 ddd (8.3, 5.6, 2.5)	79.4 (CH)	4.09 ddd (8.8, 5.7, 2.4)	79.4 (CH)
6′a	3.67 overlapped	60.7 (CH_2)	4.45 dd (11.9, 5.6)	63.5 (CH_2)	4.48 dd (11.9, 5.7)	63.5 (CH_2)
6′b	3.86 dd (12.0, 2.2)		4.65 dd (11.9, 2.5)		4.69 dd (11.9, 2.4)	
1″	4.96 s	107.6 (CH)	5.60 s	110.1 (CH)	5.74 s	108.3 (CH)
2″		85.2 (C)		87.5 (C)		92.1 (C)
3″		206.3 (C)		208.3 (C)		102.1 (C)
4″a	2.40 dd (14.8, 2.2)	39.0 (CH_2)	2.82 dd (15.2, 2.4)	41.6 (CH_2)	2.48 dd (14.0, 7.0)	36.2 (CH_2)
4″b	2.80 dd (14.8, 11.5)		3.31 dd (15.2, 11.5)		2.56 dd (14.0, 6.1)	
5″	4.17 br d (5.5)	71.3 (CH)	4.09 overlapped	73.4 (CH)	4.35 overlapped	72.7 (CH)
6″a	3.64 overlapped	62.8 (CH_2)	4.00 overlapped	65.0 (CH_2)	4.00 dd (11.0, 5.0)	66.6 (CH_2)
6″b	3.70 overlapped		4.09 overlapped		4.16 dd (11.0, 6.2)	

[a]Data were recorded at 400 MHz (^{1}H) and 100 (^{13}C) MHz, and coupling constants (*J*) in Hz were given in parentheses. [b] Data were recorded at 600 MHz (^{1}H) and 150 (^{13}C) MHz. The assignments were determined by ^{1}H, ^{13}C, COSY, HMQC, and HMBC NMR spectra.

resin (9 × 50 cm) and eluted respectively with H_2O, 40% EtOH, 70% EtOH, 95% EtOH, and 100% EtOAc (each 2.5 L) to obtain five fractions (Frs. A–E). The Fr. C (6.8 g) was chromatographed by a silica gel column (4 × 246 cm) eluted with a gradient of chloroform/methanol (MeOH) solvent system to afford twelve sub-fractions (Frs. C1 ~ C12). Of them, Fr. C10 (920 mg) was applied first by a C_{18} solid phase extraction (SPE) cartridge for further column chromatography, and then used reverse-phase high performance liquid chromatography (RP-HPLC) eluting with 60% MeOH, to obtain pure compounds **1** (12.9 mg, 0.00035%) and **3** (9.5 mg, 0.00026%). Similarly, Fr. C11 (380 mg) was undergone RP-HPLC eluted with 60% MeOH to afford **4** (10.9 mg, 0.0003%). Besides, Fr. C12 (1.4 g) was subjected to a C_{18} flash column, and eight sub-fractions (Frs. C12-1 ~ C12-8) were obtained by a gradient elution in /H_2O solvent system. Of them, **2** (21.2 mg, 0.00058%) was isolated from Fr. C12-3 (72 mg) by RP_{18}-HPLC with 55% MeOH elution.

Taimordisin A (1)

White amorphous powder; $[\alpha]^{25}_{D}$ +51.4 (*c* 0.10, MeOH); IR (KBr) ν_{max} 3382, 2946, 2875, 1710, 1634, 1454, 1382, 1259, 1073, 1039, 940 cm^{-1}; ^{1}H- (400 MHz, MeOH-d_4; 600 MHz, pyridine-d_5) and ^{13}C NMR (100 MHz, MeOH-d_4; 150 MHz, pyridine-d_5) spectroscopic data are shown in Table 1; ESIMS *m/z* 799 $[M + Na]^+$, 775 $[M-H]^-$; HR-ESI-MS *m/z* 799.4330 $[M + Na]^+$ (calcd for $C_{42}H_{64}O_{13}Na$, 11 DOU).

Taimordisin B (2)

White amorphous powder; $[\alpha]^{25}_{D}$ +40.5 (*c* 0.10, MeOH); IR (KBr)

ν_{max} 3380, 2946, 2876, 1709, 1614, 1455, 1383, 1258, 1074, 1039, 943 cm^{-1}; ^{1}H- (400 MHz, pyridine-d_5) and ^{13}C NMR (100 MHz, pyridine-d_5) spectroscopic data are shown in Table 1; ESI-MS *m/z* 817 $[M + Na]^+$, 793 $[M-H]^-$; HR-ESI-MS *m/z* 817.4363 $[M + Na]^+$ (calcd for $C_{42}H_{66}O_{14}Na$, 10 DOU).

*Taimordisin C (**3**)*

White amorphous powder; $[\alpha]^{25}_D$ +25.8 (*c* 0.43, MeOH); IR (KBr) ν_{max} 3378, 2958, 2875, 1731, 1623, 1457, 1380, 1260, 1074, 1039 cm^{-1}; ^{1}H- (600 MHz) and ^{13}C- (150 MHz) NMR spectroscopic data in pyridine-d_5 are shown in Table 2; HR-ESI-MS *m/z* 817.4373 $[M - H]^-$ (calcd. for $C_{44}H_{65}O_{14}$, 817.4366, 12 DOU).

*Taimordisin D (**4**)*

White amorphous powder; $[\alpha]^{25}_D$ +26.0 (*c* 0.40, MeOH); IR (KBr) ν_{max} 3373, 2933, 2876, 1783, 1712, 1633, 1455, 1382, 1261, 1075, 1036 cm^{-1}; ^{1}H- (600 MHz) and ^{13}C- (150 MHz) NMR spectroscopic data in pyridine-d_5 are shown in Table 2; HR-ESI-MS *m/z* 835.4499 $[M - H]^-$ (calcd. for $C_{44}H_{67}O_{15}$, 835.4485, 11 DOU).

*Acid hydrolysis of compounds **1**–**4***

Compounds **1**–**4** (1.0 mg) were hydrolyzed by treating with 2N methanolic HCl (2 mL) under the condition of reflux at 90℃ for 1 hr, respectively. Each mixture was extracted with $CHCl_3$ to give the aglycone part, and the aqueous layer was neutralized with Na_2CO_3 and filtered. The evaporated filtrates were added with 1-(trimethylsilyl) imidazole and pyridine (0.2 mL), and stirred at 60℃ for 5 min. After the reaction mixtures were dried under N_2 atmosphere, each residue was re-partitioned between $CHCl_3$ and H_2O (1:1). Each $CHCl_3$ fraction was subjected to gas chromatography (GC, column: Varian capillary column CP-chirasil-L-val for optical isomers, 25 m × 0.25 mm, 0.12 μm; column temperature, 50–150 °C, 30 °C /min, 150–180 °C, 0.8 °C /min; injector temperature, 200 °C; He carrier gas, 2.0 kg/cm^3; Mass detector, Thermo, DSQ2, electron energy, 70 eV). Under these conditions, the sugars of each reactants were identified by comparison with authentic samples: t_R (min) 30.60 (D-glucose), 30.22 (L-glucose). All the isolated glucoses from **1** − **4** were identified to be D-form.

*In vitro anti-inflammatory assay of compounds **1**–**4***

In anti-inflammatory assay, RAW 264.7 macrophage cell line was obtained from ATCC (Rockville, MD) and cultured in DMEM containing 5% heat-inactivated fetal calf serum (FCS), 100 U/mL penicillin and 100 μg/mL streptomycin and grown at 37 °C with 5% CO_2 in fully humidified air. Lipopolysaccharide (LPS)-stimulated cells (2 × 10^5 cells/well) were plated in 96-well culture plate and incubated in the presence or absence of different concentrations of analytes for 24 hr simultaneously. Analytes were dissolved in DMSO and further diluted with sterile PBS. Nitric oxide (NO)/nitrite (NO_2^-) accumulation in the medium was measured by the Griess method (Ridnour et al., 2000). Besides, the Alamar Blue cell viability assay kit (Biosource International, Nivelles, Belgium) was utilized to quantitatively measure the proliferation of RAW 264.7 macrophage cells and give the half maximal inhibitory concentration (IC_{50}) values (Al-Nasiry et al., 2007). NO production by LPS stimulation was designated as 100% for each experiment and quercetin (Sigma, 98.0% HPLC) was used as a positive control. All experiments were performed in triplicate.

Statistical analysis

SPSS (SPSS, Chicago, IL, USA) was used to perform statistical data analysis. All data are presented as the mean ± standard deviation. Groups were compared by using one-way analysis of variance (ANOVA) followed by Tukey's test of multiple comparisons. *p*-values ≤ 0.05 were considered statistically significant.

Table 2
^{1}H- and ^{13}C NMR data of taimordisins C (**3**) and D (**4**).[a]

No.	**3**[a]		**4**[a]	
	δ_H (*J*, Hz)	δ_C	δ_H (*J*, Hz)	δ_C
1a	1.67 m	21.8 (CH_2)	1.67 m	21.8 (CH_2)
1b	1.90 m		1.90 m	
2a	1.86 m	29.8 (CH_2)	1.87 m	29.7 (CH_2)
2b	1.99 m		2.00 m	
3	3.77 br s	75.5 (CH)	3.76 br s	75.5 (CH)
4		41.9 (C)		41.9 (C)
5		147.5 (C)		147.6 (C)
6	6.18 br d (4.4)	122.3 (CH)	6.15 br d (4.4)	122.2 (CH)
7	4.58 br d (5.6)	71.8 (CH)	4.54 br d (5.2)	71.6 (CH)
8	2.52 s	45.0 (CH)	2.46 s	44.9 (CH)
9		50.3 (C)		50.3 (C)
10	2.64 m	36.7 (CH)	2.61 m	36.6 (CH)
11a	1.55 m	22.6 (CH_2)	1.54 m	22.5 (CH_2)
11b	2.65 m		2.58 m	
12a	1.64 m	29.4 (CH_2)	1.56 m	29.3 (CH_2)
12b	1.64 m		1.56 m	
13		45.8 (C)		45.7 (C)
14		48.1 (C)		48.0 (C)
15a	1.52 m	34.8 (CH_2)	1.34 m	34.7 (CH_2)
15b	1.58 m		1.47 m	
16a	1.44 m	27.9 (CH_2)	1.45 m	27.5 (CH_2)
16b	1.96 m		1.79 m	
17	1.51 m	51.0 (CH)	1.45 m	51.1 (CH)
18	0.83 s	14.8 (CH_3)	0.74 s	14.8 (CH_3)
19	10.49 s	207.3 (CH)	10.46 s	207.2 (CH)
20	1.90 m	32.9 (CH)	1.81 m	32.7 (CH)
21	1.08 d (6.4)	19.2 (CH_3)	1.08 d (6.4)	19.1 (CH_3)
22a	1.18 m	43.1 (CH_2)	1.11 m	43.3 (CH_2)
22b	1.98 m		1.91m	
23	4.84 dt (2.8, 8.4)	76.0 (CH)	4.80 m	75.3 (CH)
24	5.51 br d (8.8)	127.4 (CH)	5.47 br d (8.4)	128.2 (CH)
25		134.1 (C)		133.0 (C)
26	1.66 s	25.8 (CH_3)	1.64 s	25.7 (CH_3)
27	1.73 s	18.2 (CH_3)	1.71 s	18.2 (CH_3)
28	1.12 s	27.3 (CH_3)	1.10 s	27.3 (CH_3)
29	1.43 s	26.2 (CH_3)	1.42 s	26.2 (CH_3)
30	0.76 s	18.2 (CH_3)	0.69 s	18.1 (CH_3)
1′	4.99 d (8.0)	101.8 (CH)	4.92 d (8.0)	101.8 (CH)
2′	3.98 dd (8.0, 8.0)	75.0 (CH)	3.98 m	75.0 (CH)
3′	4.27 dd (8.4, 13.4)	78.6 (CH)	4.27 m	78.6 (CH)
4′	4.24 m	71.8 (CH)	4.23 m	71.8 (CH)
5′	4.04 m	78.8 (CH)	4.00 m	78.8 (CH)
6′a	4.38 m	63.0 (CH_2)	4.38 m	63.0 (CH_2)
6′b	4.61 dd (1.2, 11.6)		4.62 br d (8.4)	
1″	5.73 br s	96.9 (CH)	5.34 s	101.4 (CH)
2″		165.5 (C)		76.5 (C)
3″	5.40 dd (8.4, 2.0)	86.2 (CH)	5.20 m	86.6 (CH)
4″	4.21 m	74.6 (CH)	4.82 m	65.7 (CH)
5″	3.92 m	77.5 (CH)	4.35 m	79.3 (CH)
6″a	4.33 dd (8.4, 11.6)	61.3 (CH_2)	4.22 m	62.9 (CH_2)
6″b	4.39 m		4.38 m	
7″a	6.28 m	112.8 (CH)	3.15 d (16.0)	42.3 (CH_2)
7″b			3.27 d (16.0)	
8″		172.8 (C)		175.8 (C)

[a]Data were recorded at 400 MHz (^{1}H) and 100 (^{13}C) MHz, and coupling constants (*J*) in Hz were given in parentheses. The assignments were determined by ^{1}H, ^{13}C, COSY, HMQC, and HMBC NMR spectra.

Results and discussion

The ethanolic extract of the fresh *M. charantia* fruits was suspended in H_2O and chromatographed on Diaion HP-20 open column successively eluting with 40%, 70%, 95% EtOH, and 100% EtOAc solvents. The 70% EtOH extract was further subjected a silica gel column and preparative RP-HPLC successfully to yield four new cucurbitane-type glycosides (**1**–**4**) (Fig. 1). The chemical structures of these compounds were elucidated by the detailed analysis of spectroscopic data including 1D, and 2D NMR, UV, IR, and HRMS experiments. All the isolated compounds were evaluated for anti-inflammatory activity through the inhibition of LPS-induced NO production in macrophage RAW264.7 cell

in vitro.

Identification of new isolated compounds

Taimordisin A (**1**), $[\alpha]^{25}_{D}$ +51.4 (*c* 0.1, MeOH), was purified and dried as pale-yellow amorphous powders. Its molecular formula $C_{42}H_{64}O_{13}$ was deduced on the basis of the pseudo-molecular ion at *m/z* 799.4330 $[M + Na]^+$ (calcd 799.4245 for $C_{42}H_{64}O_{13}Na$) analyzed by HR-ESI-MS on par with 11 degrees of unsaturation (DOU). The IR spectrum showed absorption bands indicating existence of hydroxyl (3382 cm^{-1}), carbonyl (1635 cm^{-1}), and alkene (1634 cm^{-1}) functional groups. The ^{1}H-, ^{13}C NMR, and DEPT spectra (Table 1) of **1** unambiguously demonstrated the presence of six methyls, ten methylenes (two oxymethylenes at δ_C 60.7 and 62.8), five methines, eight oxymethines, two hemiacetals, one tri-substituted double bond, one terminal olefin, five quaternary carbons (one oxygenated at δ_C 81.1), one aldehyde, and one ketone. Of which, the core structure of cucurbitane glycoside was reconstructed by these characteristic features, including multi-methyls, two oxygenated methines, one tri-substituted double bond, one aldehyde, and one monosaccharide. Next, this compound was subjected to acidic hydrolysis with 2 N methanolic HCl to free a monosaccharide, which was then determined to be a *β*-D-glucose (*β*-Glc) by HPLC against commercial sugar standards.

Based on the HMQC assignment, the planar tetracyclic skeleton of momordicine glycoside, 3-hydroxycucurbita-5-en-19-al-7-*O*-*β*-glucopyranoside, of the product **1** was elucidated by COSY and HMBC

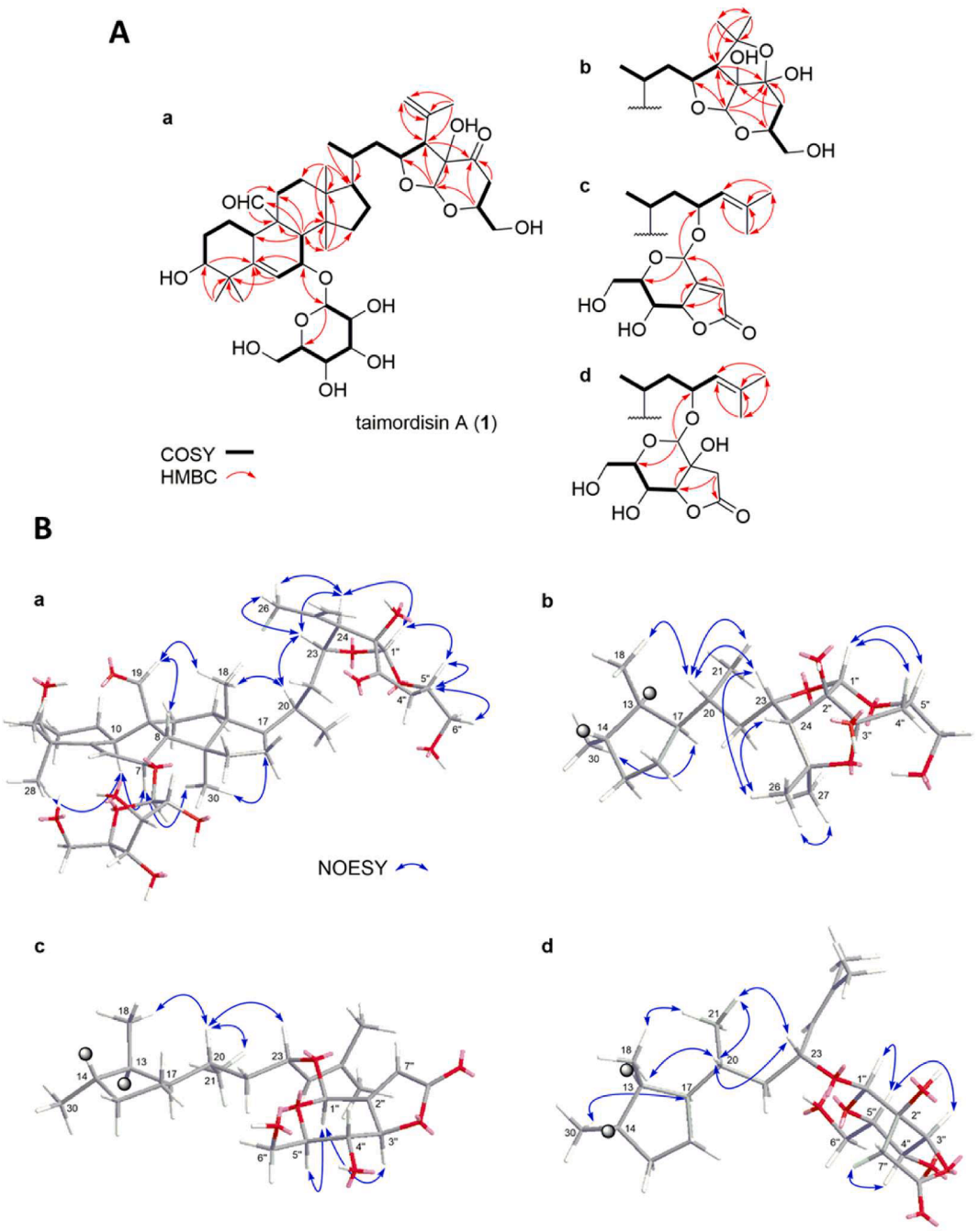

Fig. 2. 2D NMR correlations of compounds **1**–**4**. (A) a. COSY (thick lines) and selected HMBC (red arrows) correlations of **1**, and those correlations of side chain moieties of **2**–**4** (b–d). (B) Key NOESY (blue double-headed arrows) correlations of **1**, and those correlations of side chain moieties of **2**–**4** (b–d), of which the black balls replaced the tetracyclic residues. (For interpretation of the references to colour in this figure legend, the reader is referred to the web version of this article.)

correlations (Fig. 2a), in which D-glucose (C-1′−C-6′) was connected to C-7 by an *O*-linkage as the anomeric H-1′ is correlated to the oxygenated methine C-7 and likewise H-7 to C-1′. Meanwhile, the $^{1}H-^{1}H$ COSY correlations (Fig. 2A) of H_3-21/H-20/H_2-22/H-23/H-24, the HMBC correlations of H_3-26 and the olefinic H_2-27 with C-24, and the quaternary sp^2 carbon C-25 together detailed a Δ_{25}-unsaturated-C_8 side chain, which is connected between C-17 and C-20 through a C—C linkage by the HMBC correlations (Fig. 2A) from H-20 and H_3-21 to C-17. Until now, the C_6 unit (usually a glucose in almost all reported cucurbitane glycosides) along with three DOU remained further elucidation. This C_6 unit was speculated to be a deoxy-hexulose analogue based on the characteristic NMR signals of a carbohydrate anomeric carbon at δ_C 101.8 (C-1″ in pyridine-d_5), methylene carbon (C-4″ at δ_C 41.6), three oxygenated carbons (C-2″ at δ_C 87.5, C-5″ at δ_C 73.4, and C-6″ at δ_C 65.0), and a ketone (C-3″ at δ_C 208.3). In HMBC spectrum, the correlations from H-1″ to C-2″ and C-23; from H-4″ to C-2″, C-3″, C-5″, and C-6″; and from H-5″ to C-1″, C-3″, C-4″, and C-6″ confirmed that the C_6 moiety is 23-*O*-*β*-3″-dehydro-4″-deoxy-glucose. Unexpectedly, the significant HMBC correlations of H-1″ with C-24 and H-24 with C-1″, C-2″, and C-3″ indicated a new carbon–carbon bond between C-24 and C-2″, highlighting the formation of furo[2,3-*b*]pyranone by a new tetrahydrofuran ring (C-23−C-24−C-1″−C-2″) fused to the pyranose ring, leading to the establishment of the unprecedented structure of taimordisin A (**1**).

In terms of stereochemistry, the rigid tetracyclic moiety of **1** displays an identical configuration to that of regular momordicine derivatives in light of NOESY that provides unequivocal assignments. The NOE correlations (Fig. 2B) of H-3/H_3-28, H_3-29, H-10/H_3-28, H_3-30, H_{eq}-1, and H_3-30/H-7, H-17 were observed in the NOESY spectrum, indicating *α*-orientations for H-3, H-10, H-7, H-17, and H_3-30, whereas the NOE correlations of H_{ax}-1/H-19 and H-8/H-19, H_3-18 suggested *β*-orientations for CHO-19, H-8, and H_3-18. Additionally, the nuclear overhauser effects of H_3-18/H-20, H-20/H-23 and H-23/H-24, H_3-26, revealing H-20, H-23 and H-24 at the side chain towards to *β*, *β*, and *α*-directions, respectively. The chirality of H-1″ and H-5″ was determined to be *α*-position by the presence of H-1″/H-5″ and H-1″/H-24 resonances and the absence of H-23/H-1″ resonance, these NOE signals also confirmed that C-23 is attached with a *β*-Glc moiety through an oxygen bridge and therefore OH-2″ should be *α*-orientated.

Taimordisin B (**2**), $[\alpha]^{25}_{D}$ +40.5 (*c* 0.1, MeOH), has a molecular formula of $C_{42}H_{66}O_{14}$ (on par with 10 DOU) based on the HR-ESI-MS pseudo-molecular ion at *m/z* 817.4363 $[M + Na]^+$ (calcd 817.4350 for $C_{42}H_{66}O_{14}Na$). In light of similar 1D NMR to **1** (Table 1) and corresponding COSY and HMBC correlations (Fig. 2), **2** is illustrated as a congener of **1** containing 3-hydroxycucurbita-5-en-19-al-7*β*-*O*-glucopyranoside but with a different side chain. By comparing with NMR data, only did C-25, C-27, and C-3″ show apparent chemical shifting, C-25 and C-27 from δ_C 137.9 and 116.8 to 81.1 and 33.4, highlighting that the terminal olefin group (C-25 = C-27) is transformed to an oxygenated quaternary carbon (C-25) substituted with methyls (C-27 and C-26) as well as C-3″ from δ_C 208.3 to 102.1, converting a ketone to a hemiacetal in **2**, respectively. Furthermore, three DOU remained unsettled after deduction the contribution from the main momordicine glycoside moiety, implying the presence of three rings. By HMBC correlations from H_3-27 to C-24, C-25, and methyl C-26; from H_3-26 to C-24, C-25, and C-27; from H-24 to C-25, hemiacetals C-1″ and C-3″, and oxygenated quaternary carbon C-2″; from H-1″ to C-23, C-24, C-2″, C-3″, and C-5″; and from H_2-4″ to C-2″ and C-3″, a new tetrahydrofuran ring was concluded expansion to a tetrahydrofuran-adjoined pyranose bicyclic ring through the new oxygen bridge between C-25 and C-3″, disclosing an unprecedented trifuso-centro-fused ring system (Fig. 2A) which is reminiscent to tribenzotriquinacene featuring a rigid, convex–concave, C_{3v}-symmetrical molecular framework (Kuck & Seifert, 1992).

Putting these two planer structures together, the only architectural variation between **1** and **2** is the bi- and tri-cyclic ring systems, suggesting that the relative stereochemistry of **2** is identical to **1**. Apart from the ring unit at the side chain, the configurations of **2** are 3*S**, 5*E*, 7*S**, 8*S**, 9*R**, 10*R**, 13*R**, 14*S**, 17*R**, 20*R**, 23*R**, 24*R**. Likewise, the similar NOESY information (Fig. 2B) of H-1″/H-5″and H-24/H-1″ denotes the *α*-orientated H-1″, H-5″, and OH-2″, revealing that the chiral carbons of the *β*-Glc moiety in the trifuso-centro-fused ring are 1″*R**, 2″*S**, 3″*S**, and 5″*S** geometry.

Taimordisin C (**3**) was obtained as white amorphous powders with a molecular formula $C_{44}H_{66}O_{14}$ (12 DOU) by HR-ESI-MS *m/z* 817.4373 $[M - H]^-$ (calcd. for $C_{44}H_{65}O_{14}$, 817.4366). In comparison with the very kindred UV, IR, and NMR spectral data of **3** and **1**, compound **3** also holds a 3-hydroxycucurbita-5-en-19-al-7*β*-*O*-glucopyranoside module. A conventional Δ_{24}-unsaturated-C_8 side chain was then determined on the basis of the COSY correlations of H_3-21/H-20/H_2-22/H-23/H-24 and the HMBC correlations from H_3-26 and H_3-27 to trisubstituted double bond C-24 and C-25. After deduction of the above carbons, eight carbons remain awaited for assignment and could be categorized into one oxymethylene at δ_C 61.3, five methines (three oxymethines at δ_C 74.6, 77.5, and 86.2, one hemiacetal at δ_C 96.9, and one olefinic methine at δ_C 112.8), and one ester carbonyl carbon at δ_C 172.8 by analyzing the DEPT differentiation. Among them, hemiacetal C-1′′ is the anomeric carbon in a 23-*O*-linkage with a long-range correlation of H-1′′ to C-23. A short COSY fragment of H-4′′/H-5′′/H_2-6′′ (a feature of carbohydrates) and the HMBC correlations of H-1′′/C-5′′, H-3′′/C-2′′ in addition to the specific olefinic proton H-7′′/C-1′′, C-2′′, C-3′′, and C-8′′ together bring about an unpredicted furo[3,2-*c*]pyranone derivative, a glucose accessorized with an α,β-unsaturated γ-lactone ring along the C-2′′−C-3′′ bond (Fig. 2B). The ^{1}H- and ^{13}C NMR data of **3** were assigned and shown in Table 2 on the basis of HSQC, and HMBC correlations of **3**.

The stereochemistry of the momordicine glycoside moiety of **3** has a conserved configuration as that of known (23*R*)-3*β*-hydroxycucurbita-5*E*,24-dien-19-al-7*β*-*O*-glucopyranosides. The NOESY cross-peaks of H-1″/H-3″/H-5″ suggest that the 23-*O*-glucose derivative comes from a *β*-D-glucose, and H-1″, H-3″, and H-5″ are all axial position at the opposite direction of H-4″ (1″*R**, 2″*R**, 3″*S**, and 5″*R**) as shown in Fig. 2B.

Following the similar routine, by comparing the very similar UV, IR, and NMR spectral data of taimordisin D (**4**) and **3** we think that **4** was a hydrolyzed homologue of compound **3**, which was confirmed by the differences between the molecular formulas of **4** [$C_{44}H_{68}O_{15}$ (11 DOU) deduced from HR-ESI-MS *m/z* 835.4499 $[M - H]^-$ (calcd. for $C_{44}H_{67}O_{15}$, 835.4485)] and **3** ($C_{44}H_{66}O_{14}$, 12 DOU). By analyzing the ^{13}C and DEPTs spectra of **4**, only two carbon resonances were found to show obvious chemical shift's migration, δ_C 165.5 (C) and 112.8 (CH) to 76.5 (C) and 42.3 (CH_2), indicating that an olefin group was hydrolyzed. Furthermore, the HMBC correlations (Fig. 2B) of H_2-7″/C-3″, C-8″, and H-3″/C-2″ shed that the hydration reaction has occurred on the C-2″=C-7″ double bond. Thereby, 23-*O*-linked 5/6-fused bicyclic ring in **4** is determined as 3a,4,7-trihydroxy-6-(hydroxymethyl)-tetrahydro-4*H*-furo[3,2-*c*]pyran-2(3*H*)-one.

The optical specific rotation of **4** is $[\alpha]^{25}_{D}$ +26.0 (*c* 0.40, MeOH) with a positive value and of dextrorotary as that of compounds **1**–**3**, indicating that hydration did not change the relative stereochemistry of **4**. The 23-*O*-furo[3,2-*c*]pyranone in **4** is also originated from a *β*-D-glucose, the characteristic configurations of 1″*R**, 2″*R**, 3″*S**, and 5″*R** are also adopted here, except the chirality of C-4″ that is altered from *S** to *R** due to the priority switch by the adjacent saturated lactone (C-2′′−C-3′′−O–C-8′′−C-7′′). Therefore, the stereochemistry assignment for **4** is completed and the NOESY correlations of the side chain moiety in **4** is illustrated (Fig. 2B).

*Proposed biosynthetic pathways of taimordisins A–D (**1**–**4**)*

Because RNA-seq analysis by next generation sequencing has pressed ahead the progress of biosynthesis of plants' secondary metabolites in recent years, different OSCs have been identified governing formation of given types of triterpenoids and steroids. Like canonical triterpenoids,

the first committed step in cucurbitacins biosynthesis is the cyclization of 2,3-oxidosqualene by a cucurbitadienol synthase (an OSC), and the cyclized product, cucurbitadienol, is subject to subsequent oxidation and glycosylation by cytochrome P450s and UDP-glycosyltransferases, respectively (Shang et al., 2014; Cui et al., 2020). Based on reported momordicine glycosides that possess the same core aglycone (3,7,23-trihydroxycucurbita-5,24-dien-19-al) but with various levels of glycosylation at C-7 and C-23, for example, momordicines I (**5**, 7,23-diol), II (**6**, 23-*O*-Glc), IV (**7**, 7-*O*-Glc) (Mekuria et al., 2006), and 3-hydroxycucurbita-5,24-dien-19-al-7,23-di-*O*-*β*-glucopyranoside (**8**) (Ma et al., 2010), we hypothesized that compound **8** is the common precursor of taimordisins A–D (**1**–**4**), and the possible biosynthetic pathways of **1** and **2** are shown in Fig. 3, in which the linear side chain is folded to rare but fascinating 5/6/5-fused heterocyclic ring system. As well, **3** and **4** is added with an extra C_2 unit to form the uncommon but naturally-occurring furo[3,2-*c*]pyranone scaffold.

Having been glycosylated at 23-OH of momordicine IV, compound **8** is connected with the 23-*O*-*β*-D-glucopyranose moiety, then this hexose is oxidized to give rise to 2-keto-glucopyranose [the reaction could be catalyzed by pyranose dehydrogenase (Graf et al., 2013) or pyranose 2-oxidase (Wongnate & Chaiyen, 2013)]. For the biosynthesis of **1** and **2**, the synthesis is directed to route **a**: Given relatively high acidity at alpha carbon (Cα-2″, is more acidic than a typical carbon) of 2-keto-glucopyranose, the pyranose allows enolization, dehydration and enol-keto tautomerization to take place, thus leading to the formation of 2,3-diketo-4-deoxy-glucopyranose. Next, an intermolecular carbonyl-ene reaction may ensue, whereby the novel skeleton of **1** is yielded with a newly formed carbon–carbon bond (C-24–C-2″). This intermolecular carbonyl-ene reaction accounts for the configurations of *syn*-form ring junction in **1** and the *α-trifuso*-bridgehead in **2**, in agreement with the concerted mechanism favoring the *exo* position of the bulky substituent in the cyclic transition state (Achmatowicz & Bialecka-Florjanczyk, 1996). Then, a further oxa-Michael addition triggers a cascade of nucleophilic and electrophilic attacks at Cα-2″ and olefinic C-25, respectively, bringing another tetrahydrofuran ring to **2**. Thereby, the architecture of **2** contains a synthetically formidable trifuso-centro-fused asymmetric alicyclic unit with the IUPAC name of tetrahydro-2*H*,4a*H*-1,4,7-trioxacyclopenta[*cd*]indene-2a[1],4a(7a*H*)-diol.

Compounds **3** and **4** may likewise be derived from **8** following the "b" route. First, the 3-OH group of 2-keto-glucopyranose is acetylated [the additive C_2 unit of acetyl group C-7″−C-8″ may be yielded by pyruvate dehydrogenase complex, PDC (Patel et al., 2014)], where the acetyl group is enolized to form an enol nucleophile, which attacks ketone C-2″ and triggers an annulation reaction via an intermolecular aldol-type cyclization forming a five-membered β-hydroxy γ-butyrolactone moiety **4** with a new carbon–carbon bond (C-2″−C-7″). Next, 4,7-dihydroxy-6-(hydroxymethyl)-7,7a-dihydro-4*H*-furo[3,2-*c*]pyran-2(6*H*)-one is formed after dehydration, where the momordicine glycoside with a 5/6-fused bicyclic ring is compound **3**.

The oxidation of glucose to 2-keto-glucopyranose is often catalyzed by pyranose dehydrogenase or pyranose 2-oxidase, that belong to the pyranose oxidase family a FAD-dependent oxidoreductase in the glucose-methanol-choline superfamily of oxidoreductases specific to bacteria and fungi. It oxidizes D-glucose as well as other monosaccharides at the C2 position concomitant with formation of hydrogen peroxide (Abrera et al., 2020). The addition of the C_2 acetyl unit (C-7″−C-8″) may be implemented by PDC. Given these facts, it seemed very possible that these two furo[3,2-*c*]pyranone-containing compounds **3** and **4** are metabolized products of a notorious fungal plant pathogen, *Fusarium oxysporum*, which can cause vascular wilt disease of cucurbits (Namiki et al., 1994; Li et al., 2020) or by a different fungal pathogen *Aspergillus nidulans* (also called *Emericella nidulans*), a saprophytic Ascomycete that can secrete cell wall-degrading enzymes for plant fungal infections (Dean & Timberlake, 1989). One way or another, these two pathogenic fungi contain PDCs likely responsible for the addition of this essential acetyl group to trigger subsequent biotransformation (Ries et al., 2018; Chidi et al., 2020).

In vitro anti-inflammatory activity of taimordisins A–D (1–4)

The anti-inflammatory activity of taimordisins A−D (**1**–**4**) was examined using the NO-release assay on LPS-stimulated murine macrophages RAW 264.7 cells (24 hr incubation). All four compounds exhibit moderate beneficial effects on inhibition of NO production (59.5–88.5%) with IC_{50} values of 21.9–14.9 μM (Fig. 4). Similarly, all of them show high cell viability, implying that compounds **1**–**4** possess favorable cell protection activity likely scavenging extra NO accumulation, in which **3** shows strongest NO-scavenging activity. Moreover, compounds **1**–**4** were examined for antiproliferative activity against MCF-7 (human breast adenocarcinoma), Doay (human human medulloblastoma), HEp-2 (human laryngeal carcinoma), and WiDr (human colon adenocarcinoma) tumor cell lines in vitro, while these four isolates

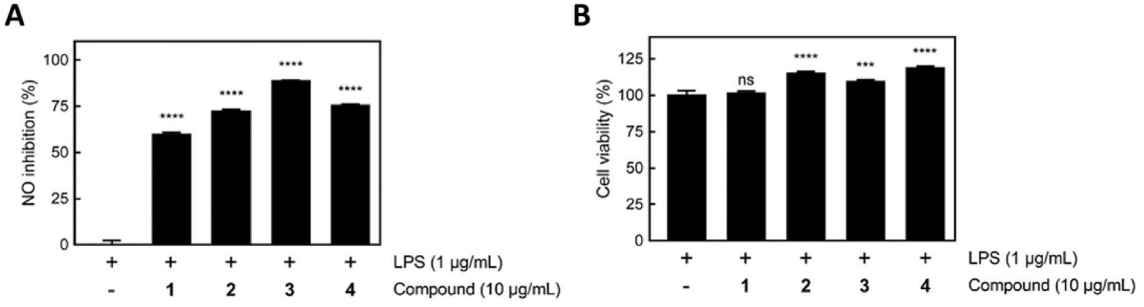

C

Compound	Anti-NO (%)[a, b]	Cell viability (%)[a, b]	IC_{50} (μM)[c]
- (LPS only)	0.00 ± 2.46	100.00 ± 3.05	----
1	59.50 ± 1.30	101.40 ± 1.42	21.90 ± 0.68
2	72.20 ± 0.96	115.00 ± 1.21	17.40 ± 0.31
3	88.50 ± 0.67	109.20 ± 1.47	14.90 ± 0.77
4	75.30 ± 0.78	118.60 ± 1.22	17.00 ± 0.48

[a] Cells were treated with LPS (1 μg/mL) or in combination with tested agents for 24h. [b] Cell lines: RAW 264.7 mouse monocyte/macrophage. [c] IC_{50}: Inhibitory concentration 50%. All values are presented as mean ± SD (n = 3).

Fig. 3. (A) NO inhibition and (B) cell viability were assessed by using Griess and Alamar blue assays, respectively. RAW 264.7 cells were with **1**–**4** (10 μg/mL) or vehicle (DMSO) in the presence of LPS (1 μg/mL) for 24 hr. Data are representative of three independent experiments (mean ± S.D.) ns, not significant; ***$P < 0.001$, ****$P < 0.0001$ compared to LPS-stimulated control. (C) Table of inhibitory results of NO production by **1**–**4**.

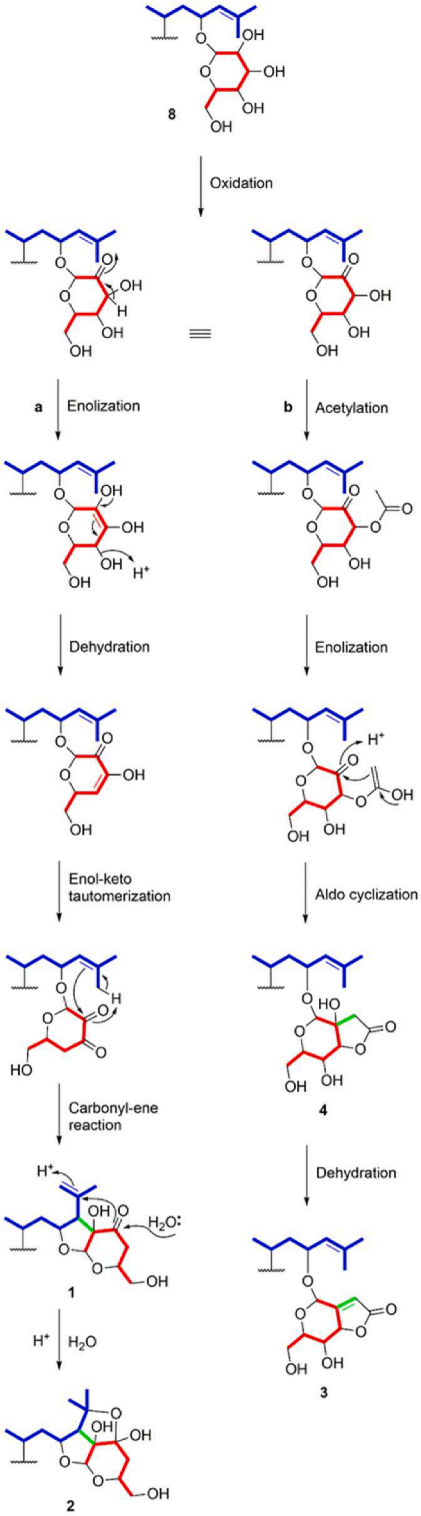

Fig. 4. Proposed biosynthetic Pathways of **1** and **2** (route a) as well as **3** and **4** (route b).

show no anti-cancer effect (data not shown) in consistence with MC used as TCM, which is well established to do with bitter flavor (cold property), nontoxicity, and relief of fatigue (Chen et al., 2015). Concerning antimicrobial activities, various fractions of MC extracts showed no harm to microbials (Khan & Omoloso, 1998; Villarreal-La Torre et al., 2020), indirectly suggesting that cucurbitacins as an adjuvant in TCM are nonpoisonous and could be metabolized by microorganisms, so that compounds **1**–**4** are likely the metabolites of microorganisms.

Conclusions

To the best of our knowledge, the identification of the trifuso-centro-fused skeleton is unprecedented as they have never been reported. The closest structures are streptoglycerides (Choi et al., 2018) and machilusides (Liu et al., 2011) respectively from marine Actinomycete *Streptomyces* species and *Machilus yaoshansis*. We believed that taimordinsins A (**1**) and B (**2**) each with a bicyclic and tricyclic unit are unusual products likely as a result of plant-endophyte interaction, because neither sugar dehydrogenase nor pyranose 2-oxidase were ever found in the *Momordica charantia* gene library, while they prevailingly exist in microbes. Likewise, 23-*O*-*β*-D-glucose in taimordisins C (**3**) and D (**4**) may be metabolized by microbial PDCs, because furo-pyranone-containing natural products are usually found in fungi. For instance, phellifuropyranone A was isolated from fruit bodies of wild fungus *Phellinus linteus* (Kojima et al., 2008), where relevant complexes were identified not only in bacteria, fungi, yeasts but also in plants and mammals. Given that the fresh bitter gourds that we collected were pesticide-free cultivated in conjunction with analysis against chromosome/enzyme database, we think that compounds **1**–**4** containing furo[2,3-*b*]pyranone or furo[3,2-*c*]pyranone moieties are the products metabolized by fungal plant pathogens, *Fusarium oxysporum* or *Aspergillus nidulans* (also called *Emericella nidulans*).

Concerning possible medicinal utilizations, these four novel triterpene glycosides from MC were examined for their anti-inflammatory and anti-cancer activities. The results suggest that taimordisins A–D (**1**–**4**) are safe with favorable anti-inflammatory activity but having no anti-cancer activity. Natural products are diverse because of diverse organisms; the diversification can be further multiplied as exemplified here through cross-interaction with species from other domains of life. Bio-reactions akin to the present example could occur in other systems, where new metabolites with novel chemical structures and unexpected biological activities await one's exploration, which is always fascinating and full of surprises.

Declaration of Competing Interest

The authors declare that they have no known competing financial interests or personal relationships that could have appeared to influence the work reported in this paper.

Acknowledgements

This work was supported by the Ministry of Science and Technology, Republic of China (MOST 104-2320-B-077-006-MY3 and MOST 103-2320-B-039-009-MY3). The authors thank the members of the Y.H. Kuo and T.L. Li Laboratories who assisted in and supported this study.

Appendix A. Supplementary data

Supplementary data to this article can be found online at https://doi.org/10.1016/j.fochx.2022.100286.

References

Abdelwahab, S. I., Hassan, L. E. A., Sirat, H. M., Yagi, S. M. A., Koko, W. S., Mohan, S., … Hadi, A. H. A. (2011). Anti-inflammatory activities of cucurbitacin E isolated from *Citrullus lanatus* var. *citroides*: Role of reactive nitrogen species and cyclooxygenase enzyme inhibition. *Fitoterapia, 82*, 1190–1197. https://doi.org/10.1016/j.fitote.2011.08.002

Abrera, A. T., Sützl, L., & Haltrich, D. (2020). Pyranose oxidase: A versatile sugar oxidoreductase for bioelectrochemical applications. *Bioelectrochemistry, 132*, Article 107409. https://doi.org/10.1016/j.bioelechem.2019.107409

Achmatowicz, O., & Bialecka-Florjanczyk, E. (1996). Mechanism of the carbonyl-ene reaction. *Tetrahedron, 52*, 8827–8834. https://doi.org/10.1016/0040-4020(96)00424-3

Akihisa, T., Higo, N., Tokuda, H., Ukiya, M., Akazawa, H., Tochigi, Y., … Nishino, H. (2007). Cucurbitane-type triterpenoids from the fruits of *Momordica charantia* and their cancer chemopreventive effects. *Journal of Natural Products, 70*, 1233–1239. https://doi.org/10.1021/np068075p

Al-Nasiry, S., Geusens, N., Hanssens, M., Luyten, C., & Pijnenborg, R. (2007). The use of Alamar Blue assay for quantitative analysis of viability, migration and invasion of choriocarcinoma cells. *Human Reproduction, 22*, 1304–1309. https://doi.org/10.1093/humrep/dem011

Bao, B., Chen, Y. G., Zhang, L. Y., Xu, L. N., Wang, X., Liu, J., & Qu, W. (2013). *Momordica charantia* (bitter melon) reduces obesity associated macrophage and mast cell infiltration as well as inflammatory cytokine expression in adipose tissues. *PLoS ONE, 8*, Article e84075. https://doi.org/10.1371/journal.pone.0084075

Chao, C. Y., Sung, P. J., Wang, W. H., & Kuo, Y. H. (2014). Anti-inflammatory effect of *Momordica charantia* in sepsis mice. *Molecules, 19*, 12777–12788. https://doi.org/10.3390/molecules190812777

Chen, H. D., Guo, J., Pang, B., Zhao, L. H., & Tong, X. L. (2015). Application of herbal medicines with bitter flavor and cold property on treating diabetes mellitus. Article ID 529491 *Evidence-Based Complementary and Alternative Medicine*. https://doi.org/10.1155/2015/529491.

Chen, J. C., Chiu, M. H., Nie, R. L., Cordell, G. A., & Qiu, S. X. (2005). Cucurbitacins and cucurbitane glycosides: Structures and biological activities. *Natural Product Reports, 22*, 386–399. https://doi.org/10.1039/b418841c

Chidi, N. I., Adekunle, A. A., Samuel, T. O., & Eziashi, E. I. (2020). Molecular identification of secreted effector genes involved in African *Fusarium oxysporum* f.sp. *elaeidis* strains pathogenesis during screening nigerian susceptible and tolerant oil palm (*Elaeis guineensis* Jacq.) genotypes. *Frontiers in Cellular and Infection. Microbiology, 10*, Article 552394. https://doi.org/10.3389/fcimb.2020.552394

Choi, B. K., Park, S. Y., Choi, D. K., Shin, B., Shin, Y. H., Oh, D. C., … Shin, H. J. (2018). Streptoglycerides A−D with a rare 6/5/5 tricyclic ring skeleton from a marine actinomycete *Streptomyces* species. *Organic Letters, 20*, 6037–6040. https://doi.org/10.1021/acs.orglett.8b02411

Cui, J. J., Yang, Y., Luo, S. B., Wang, L., Huang, R. K., Wen, Q. F., … Hu, K. L. (2020). Whole-genome sequencing provides insights into the genetic diversity and domestication of bitter gourd (*Momordica* spp.). *Horticulture Research, 7*, 85. https://doi.org/10.1038/s41438-020-0305-5

Dean, R. A., & Timberlake, W. E. (1989). Production of cell wall-degrading enzymes by *Aspergillus nidulans*: A model system for fungal pathogenesis of plants. *The Plant Cell, 1*, 265–273. https://doi.org/10.1105/tpc.1.3.265

Graf, M. M. H., Bren, U., Haltrich, D., & Oostenbrink, C. (2013). Molecular dynamics simulations give insight into D-glucose dioxidation at C2 and C3 by Agaricus meleagris pyranose dehydrogenase. *Journal of Computer-Aided Molecular Design, 27*, 295–304. https://doi.org/10.1007/s10822-013-9645-7

Huang, H. T., Zhang, L. J., Huang, H. C., Hwang, S. Y., Wu, C. L., Lin, Y. C., … Kuo, Y. H. (2020). Cucurbitane-type triterpenoids from the vines of *Momordica charantia* and their anti-inflammatory activities. *Journal of Natural Products, 83*, 1400–1408. https://doi.org/10.1021/acs.jnatprod.9b00592

Jia, S., Shen, M. Y., Zhang, F., & Xie, J. H. (2017). Recent advances in *Momordica charantia*: Functional components and biological activities. *International Journal of Molecular Sciences, 18*, 2555. https://doi.org/10.3390/ijms18122555

Khan, M. R., & Omoloso, A. D. (1998). *Momordica charantia* and *Allium sativum*: Broad spectrum antibacterial activity. *Korean Journal of Pharmacognosy, 29*, 155–158.

Kojima, K., Ohno, T., Inoue, M., Mizukami, H., & Nagatsu, A. (2008). Phellifuropyranone A: A new furopyranone compound isolated from fruit bodies of wild *Phellinus linteus*. *Chemical and Pharmaceutical Bulletin, 56*, 173–175. https://doi.org/10.1248/cpb.56.173

Kuck, D., & Seifert, M. (1992). Benzoanellated centropolyquinanes, 12. trifuso-centrotetraindan - Two syntheses of a new centropolyindan. *Chemische Berichte, 125*, 1461–1469. https://doi.org/10.1002/cber.19921250624

Li, P. F., Zhu, N. L., Hu, M. G., Wu, H. F., Yu, T., Wu, T. Y., … Xu, X. D. (2017). New cucurbitane triterpenoids with cytotoxic activities from *Hemsleya penxianensis*. *Fitoterapia, 120*, 158–163. https://doi.org/10.1016/j.fitote.2017.06.009

Li, X. F., Tian, Y. H., Peng, H. Y., He, B. L., & Gao, K. X. (2020). Isolation, screening and identification of anantagonistic actinomycetes to control *Fusarium* wilt of *Momordica charantia*. *Ying Yong Sheng Tai Xue Bao, 31*, 3869–3879. https://doi.org/10.13287/j.1001-9332.202011.036

Liaw, C. C., Huang, H. T., Lui, H. K., Lin, Y. C., Zhang, L. J., Wei, W. C., … Kuo, Y. H. (2022). Cucurbitane-type triterpenoids from the vines of *Momordica charantia* and their anti-inflammatory, cytotoxic, and antidiabetic activity. *Phytochemistry, 195*, Article 113026. https://doi.org/10.1016/j.phytochem.2021.113026

Liu, M. T., Gan, M. L., Lin, S., Zhang, Y. L., Zi, J. C., Song, W. X., … Shi, J. O. (2011). Machilusides A and B: Structurally unprecedented homocucurbitane glycosides from the stem bark of *Machilus yaoshansis*. *Organic Letters, 13*, 2856–2859. https://doi.org/10.1021/ol200854k

Ma, J., Whittaker, P., Keller, A. C., Mazzola, E. P., Pawar, R. S., White, K. D., … Rader, J. I. (2010). Cucurbitane-type triterpenoids from *Momordica charantia*. *Planta Medica, 76*, 1758–1761. https://doi.org/10.1055/s-0030-1249807

Manabe, M., Takenaka, R., Nakasa, T., & Okinaka, O. (2003). Induction of anti-inflammatory responses by dietary *Momordica charantia* L. (bitter gourd). *Bioscience, Biotechnology, and Biochemistry, 67*, 2512–2517. https://doi.org/10.1271/bbb.67.2512

Mekuria, D. B., Kashiwagi, T., Tebayashi, S. I., & Kim, C. S. (2006). Cucurbitane glucosides from *Momordica charantia* leaves as oviposition deterrents to the leafminer, *Liriomyza trifolii*. *Zeitschrift für Naturforschung C, 61*, 81–86. https://doi.org/10.1515/znc-2006-1-215

Namiki, F., Shiomi, T., Kayamura, T., & Tsuge, T. (1994). Characterization of the formae speciales of *Fusarium oxysporum* causing wilts of cucurbits by DNA fingerprinting with nuclear repetitive DNA sequences. *Applied and Environmental Microbiology, 60*, 2684–2691. https://doi.org/10.1128/aem.60.8.2684-2691.1994

Patel, M. S., Nemeria, N. S., Furey, W., & Jordan, F. (2014). The pyruvate dehydrogenase complexes: Structure-based function and regulation. *The Journal of Biological Chemistry, 289*, 16615–16623. https://doi.org/10.1074/jbc.R114.563148

Ramalhete, C., Mulhovo, S., Molnar, J., & Ferreira, M. J. U. (2016). Triterpenoids from *Momordica balsamina*: Reversal of ABCB1-mediated multidrug resistance. *Bioorganic & Medicinal Chemistry, 24*, 5061–5067. https://doi.org/10.1016/j.bmc.2016.08.022

Ridnour, L. A., Sim, J. E., Hayward, M. A., Wink, D. A., Martin, S. M., Buettner, G. R., & Spitz, D. R. (2000). A spectrophotometric method for the direct detection and quantitation of nitric oxide, nitrite, and nitrate in cell culture media. *Analytical Biochemistry, 281*, 223–229. https://doi.org/10.1006/abio.2000.4583

Ries, L. N. A., José de Assis, L., Rodrigues, F. J. S., Caldana, C., Rocha, M. C., Malavazi, I., Bayram, Ö., & Goldman, G, H. (2018). The *Aspergillus nidulans* pyruvate dehydrogenase kinases are essential to integrate carbon source metabolism. *G3 (Bethesda), 8*, 2445–2463. 10.1534/g3.118.200411.

Shang, Y., Ma, Y. S., Zhou, Y., Zhang, H. M., Duan, L. X., Chen, H. M., … Huang, S. W. (2014). Plant science. Biosynthesis, regulation, and domestication of bitterness in cucumber. *Science, 346*, 1084–1088. https://doi.org/10.1126/science.1259215

Shibuya, M., Adachi, S., & Ebizuka, Y. (2004). Cucurbitadienol synthase, the first committed enzyme for cucurbitacin biosynthesis, is a distinct enzyme from cycloartenol synthase for phytosterol biosynthesis. *Tetrahedron, 60*, 6995–7003. https://doi.org/10.1016/j.tet.2004.04.088

Sung, J., Ho, C. T., & Wang, Y. (2018). Preventive mechanism of bioactive dietary foods on obesity-related inflammation and diseases. *Food & Function, 9*, 6081–6095. https://doi.org/10.1039/c8fo01561a

Thorat, S. S., & Kontham, R. (2021). Strategies for the synthesis of furo-pyranones and their application in the total synthesis of related natural products. *Organic Chemistry Frontiers, 8*, 2110–2162. https://doi.org/10.1039/D0QO01421D

Villarreal-La Torre, V. E., Sagástegui Guarniz, W., Silva-Correa, C., Cruzado-Razco, L., & Siche, R. (2020). Antimicrobial activity and chemical composition of *Momordica charantia*: A review. *Pharmacognosy Journal, 12*, 213–222. https://doi.org/10.5530/pj.2020.12.32

Wang, H. Y., Kan, W. C., Cheng, T. J., Yu, S. H., Chang, L. H., & Chuu, J. J. (2014). Differential anti-diabetic effects and mechanism of action of charantin-rich extract of Taiwanese *Momordica charantia* between type 1 and type 2 diabetic mice. *Food and Chemical Toxicology, 69*, 347–356. https://doi.org/10.1016/j.fct.2014.04.008

Wang, S. Z., Li, Z. L., Yang, G. L., Ho, C. T., & Li, S. M. (2017). *Momordica charantia*: A popular health-promoting vegetable with multifunctionality. *Food & Function, 8*, 1749–1762. https://doi.org/10.1039/c6fo01812b

Wongnate, T., & Chaiyen, P. (2013). The substrate oxidation mechanism of pyranose 2-oxidase and other related enzymes in the glucose–methanol–choline superfamily. *The FEBS Journal, 280*, 3009–3027. https://doi.org/10.1111/febs.12280